J Interv Card Electrophysiol (2013) 36:5–11
DOI 10.1007/s10840-012-9746-6

Thermotolerance does not reduce the size or remodeling of radiofrequency lesions in the rat myocardium

Luís Felipe dos Santos · Ednei Luíz Antonio · Andrey Jorge Serra · Gabriela Venturini · Jairo Montemor · Mieko Okada · Sergio Araújo · Paulo Tucci · Angelo de Paola · Guilherme Fenelon

Received: 29 April 2012 / Accepted: 14 September 2012 / Published online: 19 October 2012

Abstract
Purpose Late lesion extension may be involved in the genesis of delayed radiofrequency (RF) effects. Because RF lesion is thermally mediated, we hypothesized that induction of heat shock response (thermotolerance) would modulate lesion healing. We evaluated the effects of thermotolerance on the dimensions and remodeling of RF lesions in a rat model of heart failure.
Methods Wistar rats (weight 300 g) subjected to heat stress (n=22, internal temperature of 42 °C for 10 min) were compared to controls (n=22, internal temperature of 37 °C for 10 min). After 48 h (peak of HSP70 myocardial concentration), a modified unipolar RF lesion (customized catheter, tip 4.5 mm in diameter; 12 W; 10 s) was created on the left ventricular free wall. Animals were sacrificed 2 h (n=10 per group) and 4 weeks (n=12 per group) after ablation for lesion analysis. An echocardiogram was obtained at 4 weeks.
Results There was no difference between groups regarding the size of acute (controls 27±2 vs. treated 27±3 mm^2) and chronic lesions (controls 17±1 vs. treated 19±1 mm^2). Histology of lesions did not differ between groups. The echocardiogram revealed dilation of the cavities and moderate systolic dysfunction without difference between groups. Acute lesion dimensions were similar between control and treated animals over time (ablation undertaken 3, 12, 24, 48, and 72 h after hyperthermia) and also using a conventional ablation catheter (50 °C; 15 W; 10 s).
Conclusion Thermotolerance does not reduce the size or remodeling of RF lesions in the rat myocardium.

Keywords Arrhythmias · Radiofrequency · Late effects · Thermotolerance · Myocardium · Remodeling

L. F. dos Santos · E. L. Antonio · J. Montemor · M. Okada · P. Tucci · A. de Paola · G. Fenelon (✉)
Discipline of Cardiology, Paulista School of Medicine, Federal University of São Paulo,
Pedro de Toledo 781, 10th Floor (Cardiology),
São Paulo, SP 04039-032, Brazil
e-mail: guilhermefenelon@uol.com.br

A. J. Serra · G. Venturini
Department of Physical Education, Nove de Julho University,
São Paulo, Brazil

S. Araújo
Department of Pathology, Paulista School of Medicine, Federal University of São Paulo,
Rua Botucatu 740,
São Paulo, SP 04039, Brazil

1 Introduction

The mechanisms responsible for the delayed effects of radiofrequency (RF) ablation such as late atrioventricular block after atrioventricular nodal reentry tachycardia are still uncertain but seem to be related to lesion extension beyond the area of acute coagulative necrosis [1–3]. This process seems to be secondary to the inflammatory response, resulting in the extension of fibrosis to areas adjacent to those directly related to ablation and in injury to the microcirculation [1] and/or ultrastructural injury to the myocardium that surrounds the lesion [2]. Modulation of RF lesion healing may limit its late extension. Our group has demonstrated in the canine myocardium that combined treatment with corticosteroids, calcium channel blockers, and antioxidants does not reduce the size of RF lesion but attenuates the ultrastructural damage to the periphery of the lesion [4].

Reinforcement of the cellular defense mechanisms against acute stress is another not yet explored strategy that could potentially reduce late extension of RF lesion. Thermotolerance is the condition whereby a cell exposed to nonlethal

thermal stress acquires transitory resistance to previously lethal temperatures. This form of cardioprotection is mediated by heat shock proteins (HSP), the most extensively studied being HSP70, which has proved to be effective in preserving mechanical function and reducing myocardial necrosis in animal models of ischemia–reperfusion [5–7]. In contrast, in rats with infarction promoted by ligation of the anterior descending artery, thermotolerance did not reduce the size of the scar, but attenuated ventricular remodeling [6]. Since the RF lesion is of a thermal nature, we hypothesized that the induction of thermotolerance, by causing previously lethal temperatures to become nonlethal, may reduce the size of RF lesions.

The objective of the present study was to evaluate the impact of thermotolerance on the healing of RF lesions in the rat myocardium. Since in this ablation model, created by our group [8], cardiac insufficiency develops with hemodynamic characteristics similar to those of coronary occlusion infarct models, we also evaluated the effects of thermotolerance on ventricular remodeling.

2 Materials and methods

The study was approved by the Research Ethics Committee of the Federal University of São Paulo and was conducted according to institutional norms.

2.1 Experimental design

One hundred ten healthy male Wistar rats aged 7–8 weeks, weighing 295–310 g, were used. Sixteen of these animals were used for the determination of the HSP70 concentration curve in the myocardium after hyperthermia. Once the time of highest HSP70 concentration was determined, 44 animals were submitted to the custom catheter ablation protocol and divided into two groups of 22 animals each: control and treated. Forty additional animals (n=20, controls and treated) were used to assess the effect of heat shock on RF lesions over a time course and the remaining 10 animals (n=5, controls and treated) underwent the temperature-controlled ablation protocol.

2.2 Experimental preparation

The animals were anesthetized with a combination of ketamine (50 mg/kg) and xylazine (5 mg/kg) and then intubated and ventilated with positive pressure using a ventilator for rodents (Harvard Apparatus Model 683, Holliston, MS, USA).

2.3 Thermal shock

Thermotolerance was induced by the technique of immersion in a water bath as described earlier [7]. The animals were placed in a water bath cuvette with digital thermal control (LAUDA Baths 020T®, Germany). The body of the rat was submerged and the head was kept in suspension to prevent the animal from drowning and to measure its internal temperature in a constant manner with a thermometer positioned in the esophagus. Control animals were submerged in water at a temperature of 37 °C, while treated animals were submerged in water at 43 °C. Both groups were left submerged for 10 min after the target internal temperature was reached, i.e., 37 °C (±0.2 °C) in controls and 42 °C (±0.2 °C) in treated animals. Typically, target internal temperature was reached in 10–12 min, thus animals remained submerged for 20–22 min. Then, the animals were removed from the bath, carefully dried with towels to avoid hypothermia, and observed until full recovery. Thereafter, rats were kept with a normal diet at room temperatures, until the ablation procedure.

2.4 Western blotting

To validate the induction of thermotolerance, we constructed the curve of HSP70 concentration using controls (n=4) and animals sacrificed 24 (n=4), 48 (n=4), and 72 (n=4)h after hyperthermia. The hearts were removed and the fragments of the left ventricle and of the interventricular septum were stored at −80 °C until analysis by Western blotting.

Cardiac tissue was homogenized in cell lysis buffer (100 mM Tris, 50 mM NaCl, 10 mM EDTA, and 1 % Triton X-100) and with a protease inhibitor cocktail (Sigma Chemical Corp. St. Louis, MO, USA). Homogenate samples (30 μg) were submitted to 10 % SDS-PAGE. The separated proteins were transferred to a PVDF membrane (Hybond-P, Amersham Biosciences, Piscataway, NJ, USA) and the efficacy of transfer was monitored with 0.5 % Ponceau S. The membrane was incubated with a blocking buffer (5 % skim milk, 10 mM Tris–HCl, pH7.6, 150 mM NaCl, and 0.1 % Tween 20) for 2 h at room temperature and then incubated overnight at 4 °C with HSP (1:500 dilution, Abcam, USA).

After incubation, the membranes were washed three times with a secondary rabbit antibody for 1 h at room temperature (Millipore, USA). Measurements were normalized by GAPDH labeling. Western blotting revelation showed that peak HSP70 concentration in the myocardium occurred 48 h after the thermal shock (Fig. 1).

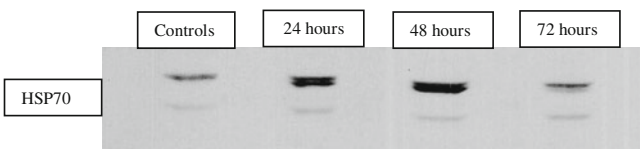

Fig. 1 Representative HSP70 concentration curve in the myocardium of control rats 24, 48, and 72 h after hyperthermia. Note the higher concentration of the protein at 48 h, followed by a sharp fall after 72 h, with a concentration similar to control values

2.5 Custom catheter ablation protocol

Forty-eight hours after hyperthermia, 44 animals were anesthetized with inhalatory halothane and subjected to the ablation procedure. After thoracotomy in the fourth left intercostal space, the heart was exposed and suspended with a customized clamp (also used as the indifferent electrode) and ablation was performed with a customized catheter with an electrode measuring 4.5 mm in diameter using a TEB® RF10 RF generator (São Paulo, Brazil) according to a technique developed by our group [8]. One ablation per animal was performed on the free wall of the left ventricle using a unipolar radiofrequency current with a fixed 12-W power for 10 s. These RF settings produce sizable left ventricular lesions without inducing severe acute heart failure.

During each application, only impedance (in ohm) was monitored and the final value was recorded for analysis since the catheter did not have a temperature sensor. The heart was then rapidly returned inside the chest, pulmonary hyperinsufflation was performed, and the chest was closed with simple sutures. The procedures were performed under sterile aseptic conditions to prevent infection.

2.6 Post-ablation period

Two hours after ablation, 20 animals (n=10, controls and treated) were sacrificed for analysis of the acute lesions. The remaining 24 animals (n=12, controls and treated) were maintained under medical-veterinary care and sacrificed 4 weeks later for the evaluation of chronic lesions.

2.7 Macroscopic analysis of the lesions

After the heart was removed, the surface of the lesion was measured with a millimeter ruler on the longitudinal and transverse axes. A thin slice of the heart was then cut transversely to the center of the lesion and incubated in a 1 % triphenyl tetrazolium chloride solution for 7 min. The depth and area of the lesion were determined using the ImageTool® software version 3.0 (UTHSCS, San Antonio, TX, USA), as illustrated in Fig. 2.

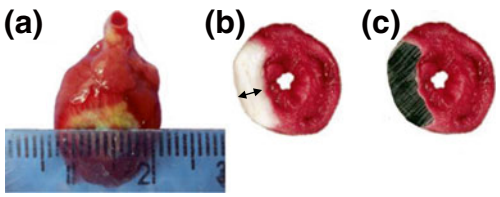

Fig. 2 Macroscopic analysis of acute lesions. (**a**) Measurement of the transverse axis of the lesion. (**b**) Measurement of lesion depth. (**c**) Calculation of the segmental area of the lesion. See text for details

2.8 Histopathological analysis of the lesions

The lesions were sectioned transversely to the center of the lesion in sections that permitted a good distinction between the necrotic area and the healthy area. The slides were stained with hematoxylin–eosin (acute group) and Masson trichrome (chronic group) and analyzed qualitatively by an experienced pathologist with emphasis on the transition area between ablated and healthy tissue.

2.9 Functional study by echocardiography

Since ventricular remodeling might influence the dimension of the chronic lesion, at the end of the 4 week follow-up, the 24 chronic animals (n=12, controls and treated) were evaluated by two-dimensional Doppler echocardiography according to a standardized technique [9] using a SONOS 5500® instrument (Hewlett Packard, Andover, MA, USA). The following data were obtained in the M mode as recommended by the American Society of Echocardiography: left atrial diameter; end-diastolic left ventricular (LV) diameter; end-systolic LV diameter; LV ejection fraction (EF) by the method of Teicholz; and the LV fractional shortening of the transverse area (FSTA).

2.10 Effect of heat shock on lesion size over a time course

In order to assess the impact of thermotolerance on RF lesion size over a time course, 40 additional animals (n=20, controls and treated) underwent the custom catheter ablation protocol 3 (n=10), 12 (n=10), 24 (n=10), and 72 (n=10)h after hyperthermia. Animals were sacrificed 2 h after ablation for macroscopic analysis of the acute lesions, as described above. Histopathological analysis was not undertaken in these animals.

2.11 Temperature-controlled RF ablation protocol

Because the custom catheter does not have a temperature sensor, we evaluated temperature-controlled RF ablation with a conventional 7-F, 4-mm solid tip ablation catheter (Biosense Webster, Diamond Bar, CA) using a TEB® RF10 RF generator (São Paulo, Brazil) in 10 additional animals (n=5, controls and treated). Ablation was conducted 48 h after hyperthermia as described above. One lesion per animal was performed on the free wall of the left ventricle using a temperature-controlled unipolar radiofrequency current (50 °C, 15 W maximum power, 10 s) with the catheter positioned perpendicular to the tissue. During each application, power (in Watts), catheter tip temperature (in degrees Celsius), and impedance (in ohm) were monitored and mean values were recorded for analysis. Animals were killed 2 h after ablation for macroscopic analysis of the acute lesions, only.

2.12 Statistical analysis

Data are reported as mean±standard deviation or mean± standard error of the mean (echocardiographic data). The categorical variables were analyzed by the Chi-square test and the continuous variables by the Student's *t* test. The level of significance was set at $P<0.05$.

3 Results

3.1 Thermal shock

The bath proceeded well in all animals, with no complications.

3.2 Radiofrequency ablation–custom catheter protocol

One ablation per animal was performed ($n=44$), using fixed power (12 W) and time (10 s). Twelve animals (27 %) manifested ventricular fibrillation immediately after application, although a brief mechanical stimulus with a clamp reestablished the rhythm. Five of these animals (41 %) belonged to the control group and seven (58 %) to the treated group (P=NS). During follow-up, two animals in each chronic group died of severe cardiac failure and were excluded from the analysis.

3.3 Macroscopic analysis

Macroscopic inspection showed an acute lesion of white color and circular morphology with defined margins, closely similar in all 20 animals of the two groups (Fig. 3). The chronic lesions were white, with sharp and well-delimited margins of closely similar appearance in all groups. The lesions were highly reproducible, with closely similar dimensions and low standard deviations, with no difference between the control and treated groups regarding the dimensions of acute and chronic lesions (Table 1).

Due to ventricular remodeling that led to dilation of the cavity and thinning of the wall, the chronic lesions showed a significantly wider transverse diameter and a smaller segmental area than the acute lesions. This phenomenon equally occurred in control and treated animals (Table 1).

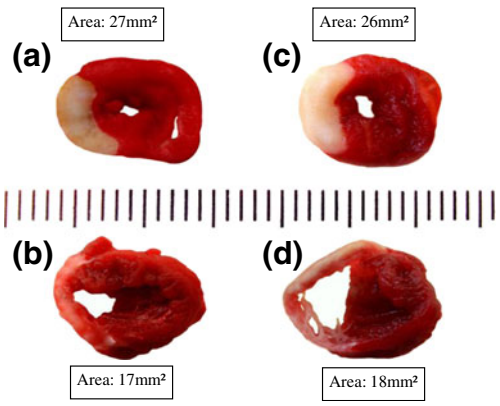

Fig. 3 Macroscopic analysis of the lesions. (**a**) Acute control. (**b**) Chronic control. (**c**) Acute treated. (**d**) Chronic treated. The segmental area of the lesion was measured using the ImageTool® software and used for group comparison. Note the consistency of the lesions in the acute and chronic groups, with no perceptible differences between groups

3.4 Histopathological analysis

In the acute lesions, there was the presence of hemorrhage, edema, and coagulative necrosis and the absence of an inflammatory infiltrate in the area of transition between ablated and healthy tissue (Fig. 4). The findings were consistent, with no differences between groups. Chronic lesions showed well delimited scars, with active fibroblasts along the transition margin. The lesions showed highly consistent fibrotic proliferation, with no difference in the progression of the healing process between groups, as shown in Fig. 4.

3.5 Echocardiography

Segmental contractile changes in the anterolateral wall of the LV, indicative of RF lesion, were observed in all animals. There was dilation of the left cardiac chambers and moderate reduction of LV systolic function. There was no difference in echocardiography measurements between groups (Table 2).

3.6 Effect of heat shock on lesion size over a time course

In addition to the 20 ($n=10$, controls and treated) acute rats ablated 48 h after heat shock (peak HSP70 concentration), 40 animals ($n=20$, controls and treated) underwent the custom catheter ablation protocol 3 ($n=10$), 12 ($n=10$), 24 ($n=10$), and 72 ($n=10$)h after hyperthermia. As shown in

Table 1 Acute and chronic lesion dimensions for the custom catheter RF ablation protocol undertaken 48 h after hyperthermia

	Transverse axis (mm)	Longitudinal axis (mm)	Depth (mm)	Area (mm^2)
Acute control ($n=10$)	9.3±0.6	9.3±0.6	2.8±0.2	27±2
Acute treated ($n=10$)	9.5±0.7	9.5±0.7	3.0±0.3	27±3
Chronic control ($n=12$)	11.0±0.9*	9.3±0.6	1.4±0.4*	17±1*
Chronic treated ($n=12$)	11.0±1.4*	9.5±1.0	1.4±0.2*	19±1*

Data are reported as mean±SD

RF radiofrequency

*$P<0.05$ as compared to the respective acute group

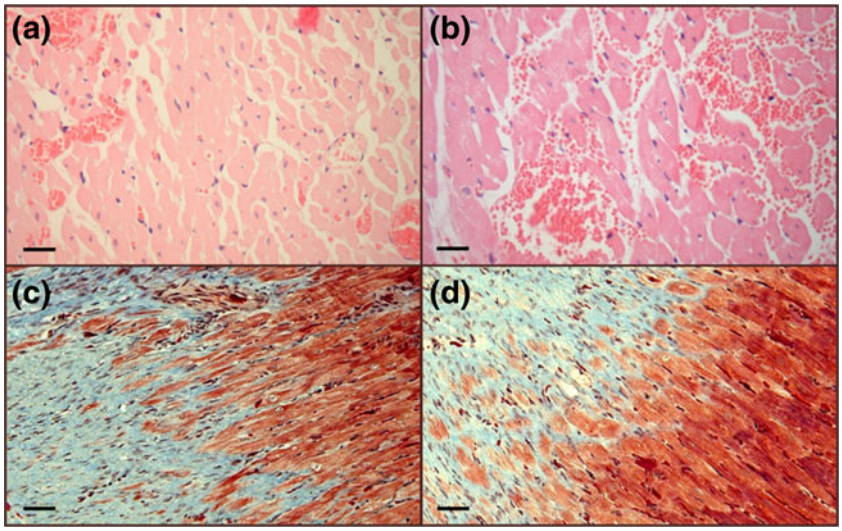

Fig. 4 Histological aspect of the transition area of acute radiofrequency lesions (**a** Control, **b** Treated) in the cardiac muscle of rats. The presence of coagulative necrosis, hemorrhage, and interstitial edema can be seen in the transition area between ablated tissue and viable tissue. *Bottom:* Images of chronic lesions (**c** Control, **d** Treated). A similar scar can be seen in the various groups, with necrosis and active fibroblasts at the periphery of the lesion and absence of an inflammatory infiltrate. Staining: **a**, **b** Hematoxylin–eosin; **c**, **d** Masson trichrome. *Bars*=50 μm

Table 3, there was no difference in acute lesion dimensions between the control and treated animals over time.

3.7 Temperature-controlled RF ablation

One temperature-controlled (50 °C; 15 W; 10 s) ablation per animal was performed (n=10) with a conventional 7-F, 4-mm tip catheter. Macroscopically, the appearance of acute lesions was similar to those created with the custom catheter, although of smaller dimensions (12 vs. 27 mm^2). Of note, there was no difference in ablation parameters and lesion size between groups (Table 4).

4 Discussion

In this model of RF ablation in the rat myocardium, we demonstrated that thermotolerance induction did not affect the dimensions of acute or chronic lesions, nor did it change their healing. Thermotolerance is the delayed protection conferred to tissue previously exposed to various types of cell aggression [6, 10, 11]. It is mediated by the activation of HSP (HSP70), which is effective in stabilizing the cell membranes during recovery from cellular stress [12, 13] and in conferring to the cell greater thermal resistance to stimuli that would normally be lethal [14, 15].

Although RF lesion is of a thermal nature, thermotolerance did not reduce the size of the lesions. The neutrality of the results cannot be attributed to methodological factors since the dimensions of the acute and chronic lesions, as well as the histopathological findings, were highly reproducible between groups. The methodology used to measure and quantify the lesion area was adequate and has been validated in

Table 2 Echocardiographic variables of chronic rats

	Control group (N=12)	Treated group (N=12)	P value
LVSD (mm)	6.5±1.6	6.4±1.3	NS
LVDD (mm)	9.6±1.1	9.8±0.9	NS
EF (%)	65±4	67±2	NS
FSTA (%)	39±3	45±3	NS
LA (mm)	5.0±4.0	4.8±1.8	NS

Data are reported as mean±SEM

LA left atrium diameter, *LVSD* left ventricular end-systolic diameter, *LVDD* left ventricular diastolic diameter, *EF* ejection fraction, *FSTA* fractional shortening of the transverse area, *NS* nonsignificant

Table 3 Acute lesion dimensions for control and treated animals undergoing custom catheter RF ablation 3, 12, 24, 48, and 72 h after hyperthermia

Group–time interval after hyperthermia	Transverse axis (mm)	Longitudinal axis (mm)	Depth (mm)	Area (mm^2)
Control–3 h (n=5)	8.7±0.2	8.9±0.1	2.3±0.1	24±2
Treated–3 h (n=5)	8.9±0.3	8.9±0.4	2.4±0.1	27±3
P value	NS	NS	NS	NS
Control–12 h (n=5)	7.4±1.6	8.7±0.2	2.4±0.1	23±2
Treated–12 h (n=5)	5.8±1.9	8.6±0.2	2.5±01	24±2
P value	NS	NS	NS	NS
Control–24 h (n=5)	9.2±0.3	8.8±0.3	2.3±0.1	22±2
Treated–24 h (n=5)	9.4±0.2	9.0±0.3	2.4±0.1	23±2
P value	NS	NS	NS	NS
Control–48 h (n=10)	9.3±0.6	9.3±0.6	2.8±0.2	27±2
Treated–48 h (n=10)	9.5±0.7	9.5±0.7	3.0±0.3	27±3
P value	NS	NS	NS	NS
Control–72 h (n=5)	9.1±0.2	8.9±0.3	2.2±0.1	25±2
Treated–72 h (n=5)	9.2±0.3	9.0±0.3	2.3±0.2	27±2
P value	NS	NS	NS	NS

Data are reported as mean±SD

NS nonsignificant, *RF* radiofrequency

Table 4 Radiofrequency application and acute lesion dimensions for temperature-controlled ablation protocol undertaken 48 h after hyperthermia

	Impedance (Ω)	Temperature (°C)	Power (W)	Transverse axis (mm)	Longitudinal axis (mm)	Depth (mm)	Area (mm^2)
Acute control (n=5)	100±16	49.6±0.2	5.2±1.6	4.5±0.5	5.1±0.5	2.0±0.1	12±2
Acute treated (n=5)	119±17	49.8±0.2	7.2±2.3	5.2±0.5	4.2±0.5	2.2±0.2	12±2
P value	NS	NS	NS	NS	NS	NS	NS

Data are reported as mean±SD

NS nonsignificant

other studies [8]. In addition, the lesions created in this model are macroscopically and histologically comparable to those created in the myocardium of dogs [4].

Several methods are used for the induction of systemic hyperthermia, such as the use of a heating blanket, heating lamps, and an infrared chamber [5, 16]. Depending on the model, the peak of HSP expression occurs 24 to 72 h after hyperthermia, returning to basal values 24 h later [5]. There is a variation in the curve of expression of these proteins that requires appropriate validation. We identified a greater expression of HSP70 48 h after hyperthermia by immersion in a water bath and not after 48–72 h as reported by Yamashita et al. [7], a fact that could be attributed to variations in the method or species. As RF ablation induces an entirely different mechanism of cell death as compared to ischemia–reperfusion injury [7], a new time course was necessary to make accurate conclusions about the effect of thermotolerance on RF lesions. To address this issue, we have demonstrated that acute lesion size does not vary between control and treated animals undergoing RF ablation 3, 12, 24, 48, and 72 h after heat shock (Table 3). In our model, HSP70 expression peaks and returns to baseline values 48 and 72 h after hyperthermia, respectively (Fig. 1).

In this ablation model, the rats consistently develop heart failure [8], so that ventricular dilation and wall thinning influence the healing of the lesions (Fig. 3). However, echocardiography showed that there was no difference in ventricular remodeling or contractile function between groups (Table 2). It is improbable that the effect of thermotolerance on lesion dimensions would have been cancelled in the exact same amount by ventricular remodeling.

As the custom catheter used in this study does not have a temperature sensor, we did not measure any temperatures during ablation. It is possible that tissue temperatures during lesion formation could be too high, thus overcoming the protective effects of thermotolerance. However, this is unlikely, since no difference in acute lesion dimensions was noted between groups during temperature-controlled (50 °C; 15 W; 10 s) ablation performed with a conventional 7-F, 4-mm tip catheter (Table 4).

The reasons for the lack of efficiency of thermotolerance in the present study are unclear, but may be related to the physiopathology of the lesions. During RF application, tissue heating decays with increasing distance from the tip of the catheter. Thus, peripheral areas around the zone of permanent tissue damage (tissue temperatures >50 °C) may undergo insufficient heating (<50 °C) to cause acute necrosis but sufficient to provoke cell damage. In this area of transition, many cells recover while others progress to necrosis and later fibrosis. Our group has reported that combined treatment with corticosteroids, antioxidants, and calcium channel blockers did not reduce the size of the lesion but attenuated the ultrastructural damage at the periphery [4]. Similarly, it is possible that thermotolerance was effective only in reducing the ultrastructural damage at the periphery of the lesions. However, this hypothesis could not be tested because electron microscopy was not available.

4.1 Clinical implications

The mechanisms underlying the delayed effects of RF have not been clarified, but it has been postulated that extension of the lesion may occur beyond the area of necrosis due to the inflammatory response associated with the process of tissue repair, resulting in fibrosis or damage to the microcirculation around the central area of necrosis. We postulated that, by elevating cell resistance to high temperatures, the cells at the periphery of the lesion would survive and therefore would not progress to necrosis and later fibrosis. In models of cardiac ischemia–reperfusion, the induction of thermotolerance minimizes fibrosis in the rat myocardium [17, 18]. However, in models of infarction due to coronary occlusion, thermotolerance did not reduce the size of the scar, although it did reduce ventricular remodeling [6]. Our study shows that in this ablation model in rats, the induction of thermotolerance is unable to minimize the dimensions of the lesion or the ventricular remodeling associated with heart failure. We may speculate that RF-induced necrosis (which occurs irreversibly within a few seconds, while ischemic necrosis takes hours to occur) may be an aggression beyond the capacity of cell protection conferred by thermotolerance. Thus, new forms of cardioprotection should be investigated in order to attenuate the delayed effects of RF ablation. However, on the other hand, thermotolerance could also decrease the therapeutic effects of RF ablation by not causing sufficient necrosis in areas of myocardium that are important for the maintenance of arrhythmias.

4.2 Limitations

The study was conducted on rats with a normal heart, and therefore, the results cannot be directly extrapolated to clinical situations. Our protocol consisted of a single induction of HSP synthesis by immersion in a water bath. Although unlikely, it is possible that other forms of thermotolerance induction [19, 20] might confer greater myocardial protection. The indices of overall systolic LV function (EF and FSTA) used do not represent the overall systolic function in hearts with regional contractile changes. However, FSTA shows a good correlation with infarct size in rats, characterizing the fact that the ventricular ejection capacity is reduced proportionally to the infarct size [8]. Finally, the electrophysiological properties of the transitional zone adjacent to the area of permanent tissue damage were not evaluated and remain undetermined.

5 Conclusion

Thermotolerance induced by systemic hyperthermia does not reduce the size or remodeling of RF lesions in the rat myocardium.

Acknowledgments This research was supported by grants from Fundação de Amparo à Pesquisa do Estado de São Paulo (LFS and GF).

References

1. Nath, S., Whayne, J. G., Kaul, S., Goodman, N. C., Jayaweera, A. R., & Haines, D. E. (1994). Effects of radiofrequency catheter ablation on regional myocardial blood flow. Possible mechanism for late electrophysiological outcome. *Circulation, 89*, 2667–2672.
2. Fenelon, G., d'Ávila, A., Malacky, T., & Brugada, P. (1995). Prognostic significance of transient complete atrioventricular block during radiofrequency ablation of atrioventricular node reentrant tachycardia. *The American Journal of Cardiology, 75*, 698–702.
3. Fenelon, G., & Brugada, P. (1996). Delayed effects of radiofrequency energy: mechanisms and clinical implications. *Pacing and Clinical Electrophysiology, 19*, 484–489.
4. Fenelon, G., Franco, M., Mora, O., Katchburian, E., & De Paola, A. A. V. (2004). Combined therapy with steroids and antioxidants prevents ultrastructural damage surrounding chronic radiofrequency lesions. *Pacing and Clinical Electrophysiology, 27*, 65–72.
5. Arnaud, C., Laubriet, A., Joyeux, M., Godin-Ribuot, D., Rochette, L., Demenge, P., et al. (2001). Role of nitric oxide synthases in the infarct size-reducing effect conferred by heat stress in isolated rat hearts. *British Journal of Pharmacology, 132*, 1845–1851.
6. Heimrath, O., Oxner, A., Myers, T., & Legare, J. F. (2009). Heat shock treatment prior to myocardial infarction results in reduced ventricular remodeling. *Journal of Investigative Surgery, 22*, 9–15.
7. Yamashita, N., Hoshida, S., Nishida, M., Igarashi, J., Aoki, K., Hori, M., et al. (1997). Time course of tolerance to ischemia–reperfusion injury and induction of heat shock protein 72 by heat stress in the rat heart. *Journal of Molecular and Cellular Cardiology, 29*, 1815–1821.
8. Antonio, E. L., Dos Santos, A. A., Araujo, S. R., Bocalini, D. S., Dos Santos, L., Fenelon, G., et al. (2009). Left ventricle radiofrequency ablation in the rat: a new model of heart failure due to myocardial infarction homogeneous in size and low in mortality. *Journal of Cardiac Failure, 15*, 540–548.
9. Kanashiro, R. M., Saraiva, R. M., Alberta, A., Antonio, E. L., Moisés, V. A., & Tucci, P. J. (2006). Immediate functional effects of left ventricular reduction: a Doppler echocardiographic study in the rat. *Journal of Cardiac Failure, 12*, 163–169.
10. Subjeck, J. R., & Shyy, T. T. (1986). Stress protein systems of mammalian cells. *American Journal of Physiology, 250*, C1–C17.
11. Snoeckx, L. H. E. H., Cornelussen, R. N., Nieuwenhoven, F. A., Reneman, R. S., & Van Der Vusse, G. J. (2001). Heat shock proteins and cardiovascular pathophysiology. *Physiological Reviews, 81*, 1461–1497.
12. Beckmann, R. P., Mizzen, L. E., & Welch, W. J. (1990). Interaction of Hsp 70 with newly synthesized proteins: implications for protein folding and assembly. *Science, 248*, 850–854.
13. Kregel, K. C., Overton, J. M., Johnson, D. G., Tipton, C. M., & Seals, D. R. (1991). Mechanism for pressor response to nonexertional heating in the conscious rat. *Journal of Applied Physiology, 71*, 192–196.
14. Laszlo, A. (1992). The effects of hyperthermia on mammalian cell structure and function. *Cell Proliferation, 25*, 59–87.
15. Kampinga, H. H. (1993). Thermotolerance in mammalian cells. Protein denaturation and aggregation, and stress proteins. *Journal of Cell Science, 104*, 11–17.
16. Donnelly, T. J., Sievers, R. E., Vissern, F. L., Welch, W. J., & Wolfe, C. L. (1992). Heat shock protein induction in rat hearts. A role for improved myocardial salvage after ischemia and reperfusion? *Circulation, 85*, 769–778.
17. Fan, C. G., Yuan, Q., Song, G., Wang, Y., Chen, G., Qian, J., et al. (2006). Small heat-shock protein Hsp20 attenuates beta-agonist mediated cardiac remodeling through apoptosis signal-regulating kinase 1. *Circulation Research, 99*, 1233–1242.
18. Cai, W. F., Zhang, X. W., Yan, H. M., Ma, Y. G., Wang, X. X., Yan, J., et al. (2010). Intracellular or extracellular heat shock protein 70 differentially regulates cardiac remodeling in pressure overload mice. *Cardiovascular Research, 88*, 140–149.
19. Ooie, T., Naohiko, T., Tetsunori, S., Tomoko, N., Masaya, A., Kunitoshi, Y., et al. (2001). Single oral dose of geranylgeranylacetone induces heat-shock protein 72 and renders protection against ischemia/reperfusion injury in rat heart. *Circulation, 104*, 1837–1843.
20. Barsheshet, A., Barshack, I., Keren, P., Keren, G., & George, J. (2008). Whole-body hyperthermia attenuates experimental autoimmune myocarditis in the rat. *Cardiovascular Pathology, 17*, 375–381.

Editorial Commentary

This is a study aimed at understanding the mechanisms of myocardial injury in tissue adjacent to lesions caused by RF ablation. One would expect that since RF lesions are produced by heat, thermotolerance would alleviate the adverse response of myocardium adjacent to RF ablation lesions. On the other hand, could thermotolerance decrease the therapeutic effects of RF ablation by not causing sufficient necrosis in areas of myocardium that are important for the maintenance of arrhythmias?